

Supporting information

Coordination polymers built up from a *s*-tetrazine derived ligand and rare earths: from a sequential dimensional expansion to organic-inorganic energy transfer

Paul Rouschmeyer,^{1,2} Nathalie Guillou,¹ Christian Serre,¹ Gilles Clavier,² Clémence Allain,^{2} Thomas Devic^{1,3*}*

¹ Institut Lavoisier, UMR 8180 CNRS - U. Versailles St. Quentin, Université Paris-Saclay, 45 avenue des Etats-Unis, 78035 Versailles, France.

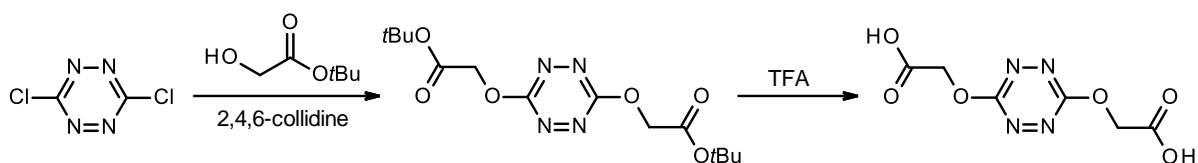
² PPSM, UMR 8531 CNRS - ENS Cachan, Université Paris-Saclay, 61 avenue du président Wilson, 94235 Cachan, France.

³ Institut des Matériaux Jean Rouxel (IMN), Université de Nantes, CNRS UMR 6502, 2 rue de la Houssinière, BP 32229, 44322 Nantes cedex 3, France.

E-mail: callain@ppsm.ens-cachan.fr, thomas.devic@cncrs-imn.fr

1. Synthesis	S2
2. X-ray diffraction (XRD) analysis	S4
3. Infrared (IR) spectroscopy	S13
4. Thermogravimetric analysis (TGA)	S15
5. Elemental analysis	S15
5. Optical experiments	S16

1. Synthesis



tert-butyl-(*s*-tetrazine)-3,6-diglycolate

tert-butyl 2-hydroacetate^[1] and 3,6-dichlorotetrazine^[2] were prepared as previously described. 1.0 g (6.6 mmol, 1 eq) of 3,6-dichlorotetrazine was dissolved in 2mL of dichloromethane, and 1.93 g (14.5 mmol, 2.2eq.) of *tert*-butyl 2-hydroacetate were added. 3.11mL (15.9 mmol, 2.4eq.) of 2,4,6-trimethylpyridine were then slowly added (caution, exothermic reaction), and the mixture was stirred at room temperature for 3 days. The mono and bis-substituted tetrazines were subsequently separated by silica gel chromatography (eluent dichloromethane : petroleum ether 1 : 1). The unreacted alcohol was finally eliminated by evaporation at 50°C under vacuum, leading to *tert*-butyl-(*s*-tetrazine)-3,6-diglycolate as a red powder. Yield: 1.30 g (3,8 mmol, 57%).

¹H NMR (400 MHz, CDCl₃): δ = 5.00 (s, 4H), 1.43(s, 18H)

¹³C NMR (100 MHz, CDCl₃): δ = 166.1, 166.0, 83.4; 65.41; 28.1

3,6-diglycolic-1,2,4,5-tetrazine acid or H₂OTz

1.30 g (3.8 mmol) of *tert*-butyl-(*s*-tetrazine)-3,6-diglycolate was dissolved in 50 mL of dichloromethane. 50 mL of trifluoroacetic acid were slowly added and the mixture was stirred at room temperature overnight. The product was then concentrated under vacuum, washed with diethylether to afford a pink powder. Yield: 0.80 g (3.4 mmol, 89%). Recrystallization in acetone afforded crystals suitable for single crystal XRD analysis (see below).

¹H NMR (400MHz, MeOD): δ = 5.14

¹³C NMR (100 MHz, MeOD): δ = 170.7, 167.4, 65.8

HRMS (ESI): calc. for C₆H₇N₄O₆ [M+H⁺] 231.0366, found 231.0364

MOFs syntheses were first carried out in autoclave reactors under static conditions. While MIL-162 prepared from nitrate salts could be obtained in a pure form, residual $\text{Ln}(\text{OH})_3$ was often found in MIL-164 and MIL-165. These two solids were ultimately obtained in a pure form when the syntheses were performed in round bottom flasks under stirring.

The optimized synthesis conditions are given below.

MIL-162(Ln) (Ln=La, Pr, Nd, Sm, Eu)

46 mg (0.2 mmol; 1eq.) of H_2OTz , 87 mg (0.2 mmol; 1eq.) of $\text{Ln}(\text{NO}_3)_3 \cdot n\text{H}_2\text{O}$ and 0.5 mL of N,N-dimethylformamide (DMF) were mixed in a 1.5 mL teflon lined autoclave reactor. The reactor was sealed and heated at 100°C for 72 hours. After cooling down to room temperature, the red solid was recovered by filtration, washed with DMF and dried in air.

MIL-164(Ln) (Ln=La, Pr, Nd, Sm) or $\text{LnCl}(\text{OTz})(\text{DMF})_2$

23 mg (0.1 mmol; 1eq.) of H_2OTz , 21 mg (0.1 mmol; 1eq.) of finely grinded $\text{Ln}(\text{OH})_3$, 33.6 μL of a 12 M aqueous HCl solution (0.4 mmol; 4 eq.) and 1 mL of DMF were mixed in a 10 mL round bottom flask. The mixture was heated at 100°C under stirring for 14 hours. After cooling down to room temperature, the red solid was recovered by filtration, washed with DMF and dried in air.

MIL-165(Tb) or $\text{TbCl}(\text{OTz})(\text{DMF})_2$

92 mg (0.4 mmol; 1eq.) of H_2OTz , 92 mg (0.4 mmol; 1eq.) of finely grinded $\text{Tb}(\text{OH})_3$, 135 μL of a 12 M aqueous HCl solution (1.6 mmol; 4 eq.) and 4 mL of DMF were mixed in a 10 mL round bottom flask. The mixture was heated at 100°C under stirring for 14 hours. After cooling down to room temperature, the red solid was recovered by filtration, washed with DMF and dried in air.

MIL-166(Tb) or $\text{Tb}(\text{OTz})_{1.5}(\text{DMF})_2$

4 mg (0.017 mmol; 1eq.) of H_2OTz was dissolved in 2.5 mL of DMF in a 10 mL round bottom flask. 10 mg (0.017 mmol; 1eq.) of MIL-165(Tb) were added, and the mixture was heated at 100°C for 14 hours. After cooling down to room temperature, the red solid was recovered by filtration, washed with DMF and dried in air.

2. X-ray diffraction (XRD) analysis

- Powder XRD

X-ray powder diffraction patterns (Figures 2, S1-S5) were measured on flat samples using a high-throughput Bruker D8 Advance diffractometer working on transmission mode, equipped with a focusing Göbel mirror producing CuK α radiation ($\lambda = 1.5418 \text{ \AA}$) and a LynxEye detector.

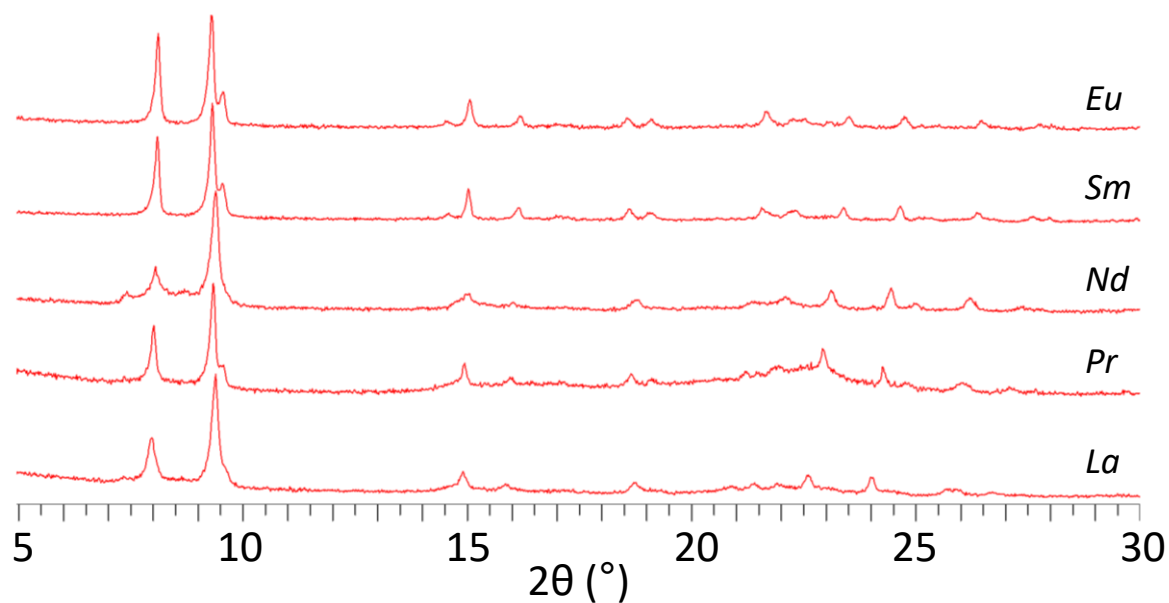


Figure S1. XRPD patterns of MIL-162(Ln) for Ln = **La**, **Pr**, **Nd**, **Sm**, **Eu** ($\lambda = 1.5418 \text{ \AA}$). Synthesis conditions: $\text{H}_2\text{OTZ} / \text{Ln}(\text{NO}_3)_3 \cdot n\text{H}_2\text{O} = 1/1$; $T = 100^{\circ}\text{C}$.

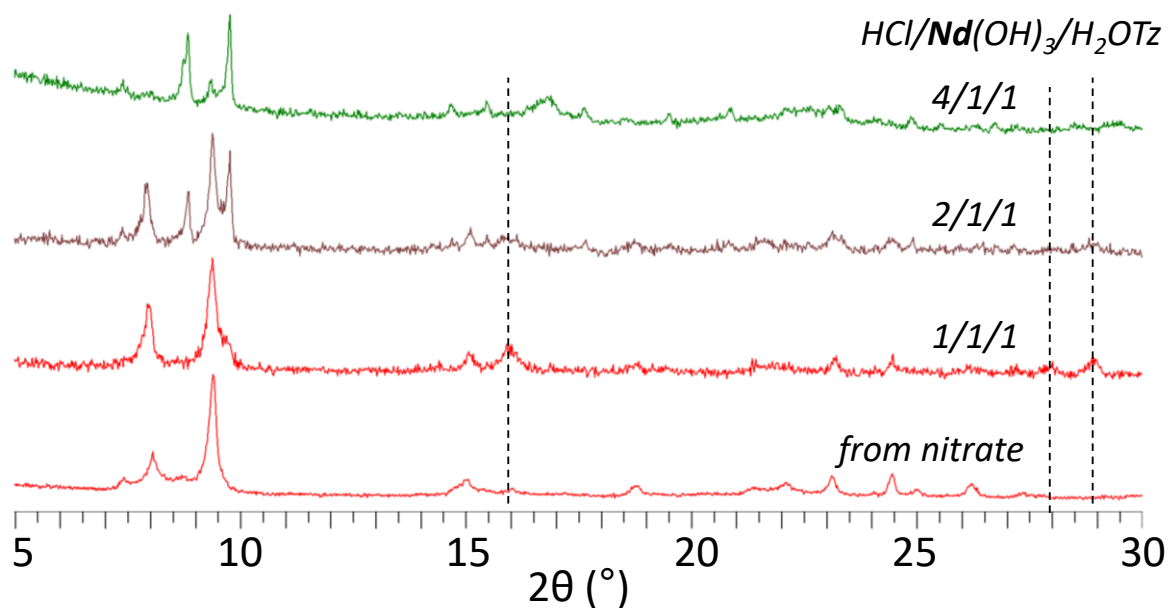


Figure S2. Effect of the variation of the HCl/Nd(OH)₃/H₂OTz (HCl/M/L) ratios on the XRPD pattern of the resulting products after reaction at 100°C in DMF ($\lambda = 1.5418 \text{ \AA}$). Red = MIL-162; green: MIL-164, brown: mixture of MIL-162 and MIL-164; dashed line: Nd(OH)₃.

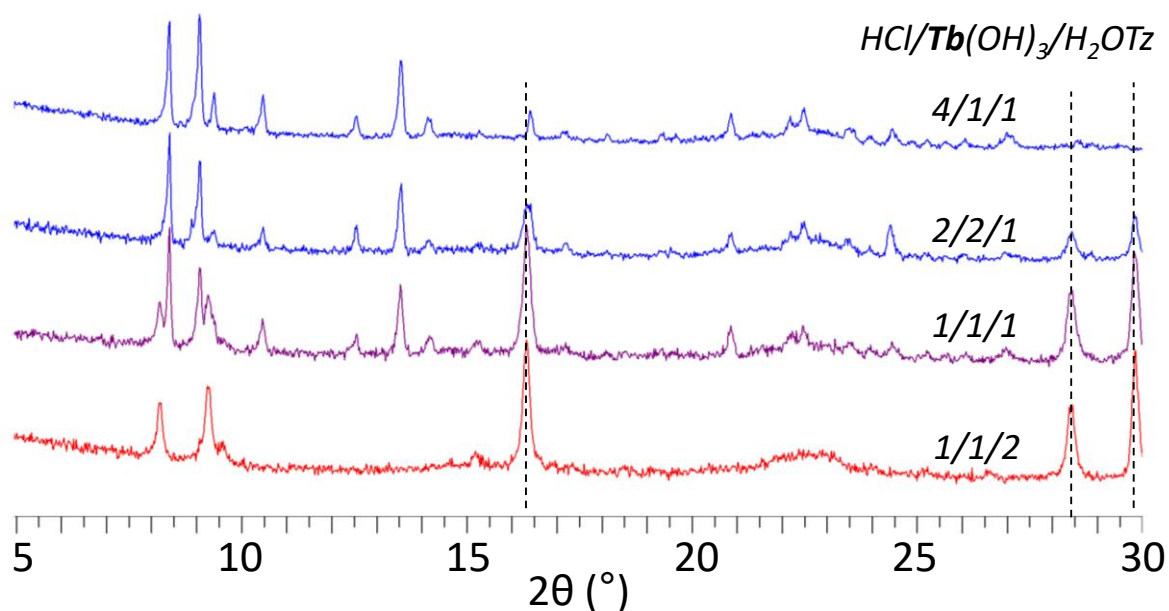


Figure S3. Effect of the variation of the HCl/Tb(OH)₃/H₂OTz (HCl/M/L) ratios on the XRPD pattern of the resulting products after reaction at 100°C in DMF ($\lambda = 1.5406 \text{ \AA}$). Red = MIL-162; blue: MIL-165, violet: mixture of MIL-162 and MIL-165; dashed line: Tb(OH)₃.

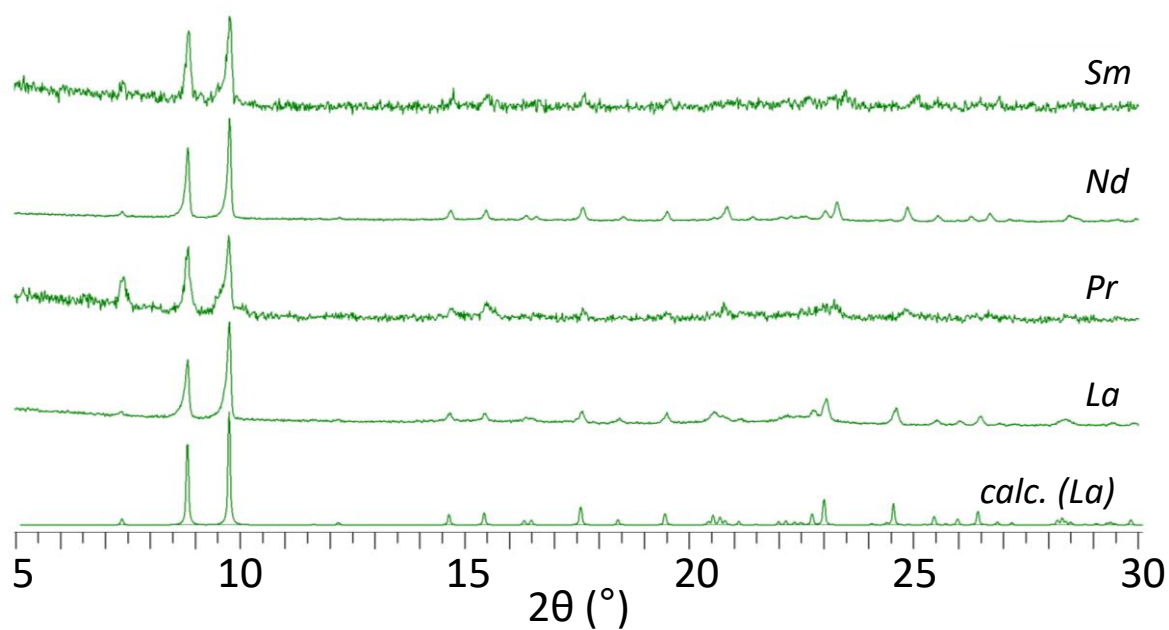


Figure S4. XRPD patterns of MIL-164(Ln) for Ln = **La**, **Pr**, **Nd**, **Sm** ($\lambda = 1.5418 \text{ \AA}$). Synthesis conditions: $\text{H}_2\text{OTZ} / \text{Ln}(\text{OH})_3/\text{HCl} = 1/1/4$; $T = 100^\circ\text{C}$.

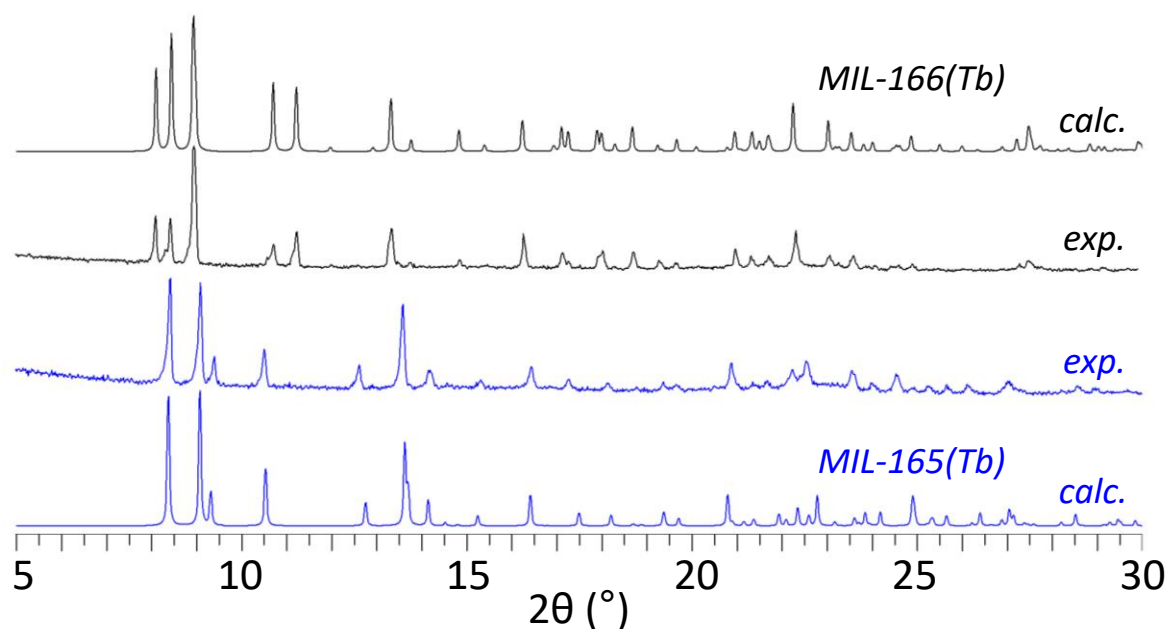


Figure S5. Comparison of the XRPD patterns of MIL-165(Tb) and MIL-166(Tb) ($\lambda = 1.5418 \text{ \AA}$).

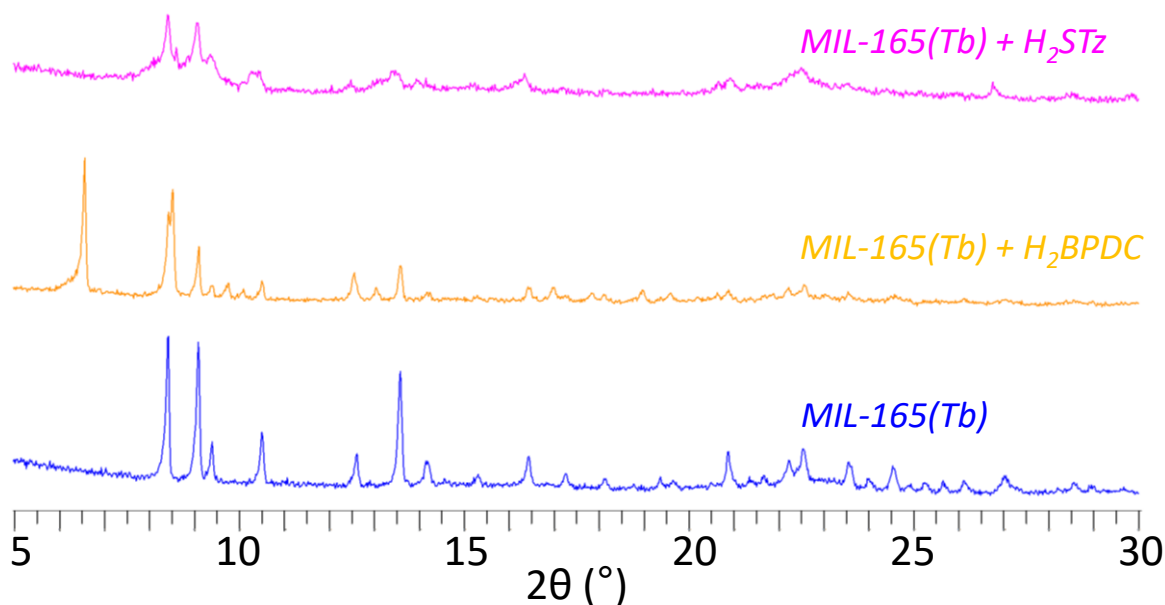


Figure S6. Comparison of the XRPD patterns of MIL-165(Tb) before and after exposure to 1 equivalent of 3,6-dithioglycolic-1,2,4,5-tetrazine acid (H₂STz) and 4,4'-biphenyldicarboxylic acid (or H₂BPDC, pink) in DMF at 100°C for 14 hrs ($\lambda = 1.5418 \text{ \AA}$).

- *Single crystal XRD*

Crystals of H₂OTz, MIL-164(La) and MIL-166(Tb) were analyzed at 293(2) K whereas MIL-165(Tb) was analyzed at 149(2) K, all using a Bruker Nonius X8 APEX diffractometer equipped with a CCD area detector. SAINT software was used to integrate and scale intensities and a semi-empirical absorption correction (SADABS) were applied on the basis of multiple scans of equivalent reflections. The structures were solved by direct methods using SHELXS-97 and refined with the full matrix least squares routine SHELXL-2014/7 or SHELX-2016/6.^[3] For of H₂OTz, MIL-164(La) and MIL-166(Tb), all non H-atoms were refined anisotropically. The weak diffracting power of the crystals of MIL-165(Tb) precluded the collection of a good dataset even at low temperature (here 149(2) K), and attempts to grow larger crystals failed. For this particular solid, few atoms were then refined isotropically, namely all non O-atoms of the solvent molecules, as well as one O and one C of the carboxylate group on OTz. For MIL-166, unbound disordered solvent molecules were discarded using the SQUEEZE procedure.^[4] H-atoms were added as rigid bodies, except the acidic H-atom in H₂OTz which was located on the difference Fourier map.

CCDC 1833257 (MIL-164(La)), 1833258 (MIL-165(Tb)), 1833259 (MIL-166(Tb)), 1833260 (H₂OTz) contain the supplementary crystallographic data for this paper. These data can be obtained free of charge from the Cambridge Crystallographic Data Centre via <http://www.ccdc.cam.ac.uk/Community/Requestastructure>. Crystallographic and refinements parameters are summarized in Table S1.

Table S1. Crystallographic data and refinement parameters for H₂OTz, MIL-164(La), MIL-165(Tb) and MIL-166(Tb).

Compound	H ₂ OTz	MIL-164(La) La(OTz)Cl(DMF) ₂	MIL-165(Tb) Tb(OTz)Cl(DMF) ₂	MIL-166(Tb) Tb(OTz) _{1.5} (DMF) ₂
Empirical formula	C ₆ H ₆ N ₄ O ₆	C ₁₂ H ₁₈ ClLaN ₆ O ₈	C ₁₂ H ₁₈ ClN ₆ O ₈ Tb	C ₁₅ H ₂₀ N ₈ O ₁₁ Tb
Formula weight (g·mol ⁻¹)	230.15	548.67	568.69	647.31
Temperature (K)	293(2)	293(2)	149(2)	293(2)
Wavelength (Å)	0.71073	0.71073	0.71073	0.71073
Crystal system	monoclinic	monoclinic	triclinic	triclinic
Space group	<i>P</i> 2 ₁ / <i>n</i>	<i>P</i> 2 ₁ / <i>c</i>	<i>P</i> -1	<i>P</i> -1
Unit cell dimensions (Å)	<i>a</i> = 4.6883(2) <i>b</i> = 10.7516(5) <i>c</i> = 8.7635(4) <i>β</i> = 95.497(3)°	<i>a</i> = 12.5822(5) <i>b</i> = 18.3349(6) <i>c</i> = 8.7335(3) <i>β</i> = 104.582(2)°	<i>a</i> = 8.443(5) <i>b</i> = 10.802(6) <i>c</i> = 11.764(8) <i>α</i> = 64.44(2)° <i>β</i> = 84.15(3)° <i>γ</i> = 89.13(4)°	<i>a</i> = 10.177(3) <i>b</i> = 11.787(6) <i>c</i> = 12.028(3) <i>α</i> = 113.632(13)° <i>β</i> = 92.422(17)° <i>γ</i> = 102.029(14)°
Volume (Å ³)	439.71(3)	1949.86(12)	962.2(10)	1280.0(7)
Z, calculated density (g·cm ³)	2,1.738	4,1.869	2,1.963	2,1.680
Adsorption coefficient (mm ⁻¹)	0.157	2.381	3.867	2.828
F(000)	236	1080	556	638
Crystal size (mm ³)	0.25 x 0.16 x 0.08	0.08 x 0.04 x 0.02	0.2 x 0.05 x 0.005	0.2 x 0.06 x 0.06
Theta range for data collection	3.007° - 38.602°	2.008° - 30.532°	2.091° - 25.118°	1.946° - 26.695°
Limiting indices	-7 ≤ <i>h</i> ≤ 8 -18 ≤ <i>k</i> ≤ 15 -14 ≤ <i>l</i> ≤ 15	-17 ≤ <i>h</i> ≤ 17 -26 ≤ <i>k</i> ≤ 25 -12 ≤ <i>l</i> ≤ 12	-10 ≤ <i>h</i> ≤ 10 -12 ≤ <i>k</i> ≤ 12 -14 ≤ <i>l</i> ≤ 13	-11 ≤ <i>h</i> ≤ 12 -13 ≤ <i>k</i> ≤ 14 -15 ≤ <i>l</i> ≤ 14

Reflections collected / unique	7504/2491 [R(int) = 0.0215]	29902/5967 [R(int) = 0.1284]	17158/3317 [R(int) = 0.3552]	9787/4966 [R(int) = 0.3080]
Refinement method	full-matrix least squares			
Data / Restraints / Parameters	2491/0/76	5967/0/257	3317/207/10	4966/320/2
Goodness of fit on F ²	1.088	1.012	0.949	0.845
Final R indices [I > 2σ(I)]	R1 = 0.0453 wR2 = 0.1337	R1 = 0.0594 wR2 = 0.0887	R1 = 0.1032 wR2 = 0.2093	R1 = 0.0603 wR2 = 0.1053
R indices (all data)	R1 = 0.0617 wR2 = 0.1479	R1 = 0.1369 wR2 = 0.1129	R1 = 0.2253 wR2 = 0.2674	R1 = 0.1786 wR2 = 0.1403
Largest diff peak and hole (e·Å ⁻³)	0.409 and -0.254	1.024 and -1.264	1.024 and -1.264	1.390 and -1.609

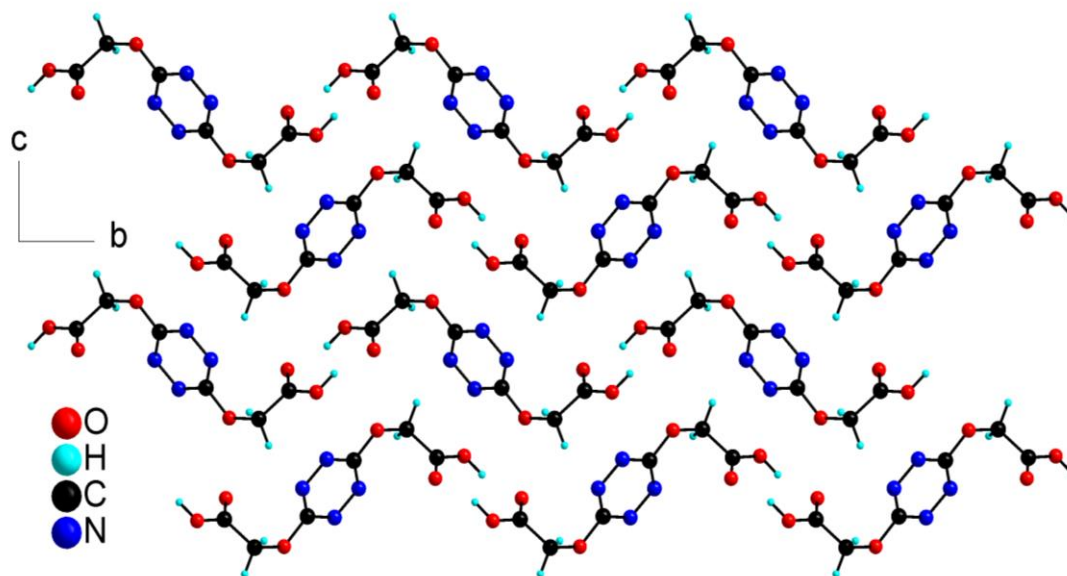


Figure S7. Crystal structure of H₂OTz.

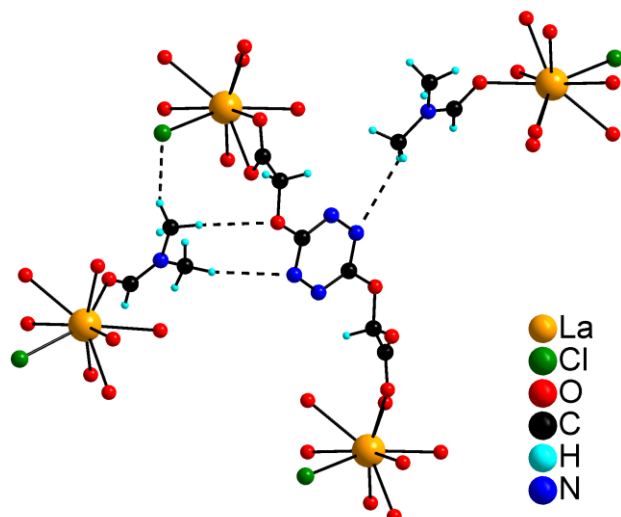


Figure S8. Short ($< 3 \text{ \AA}$) intermolecular contacts in MIL-164(La).

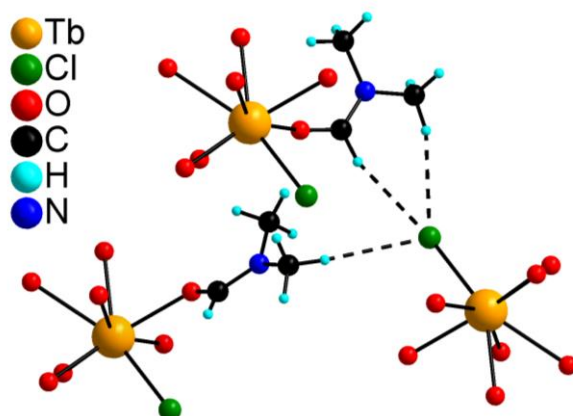


Figure S9. Short ($< 3 \text{ \AA}$) intermolecular contacts in MIL-165(Tb).

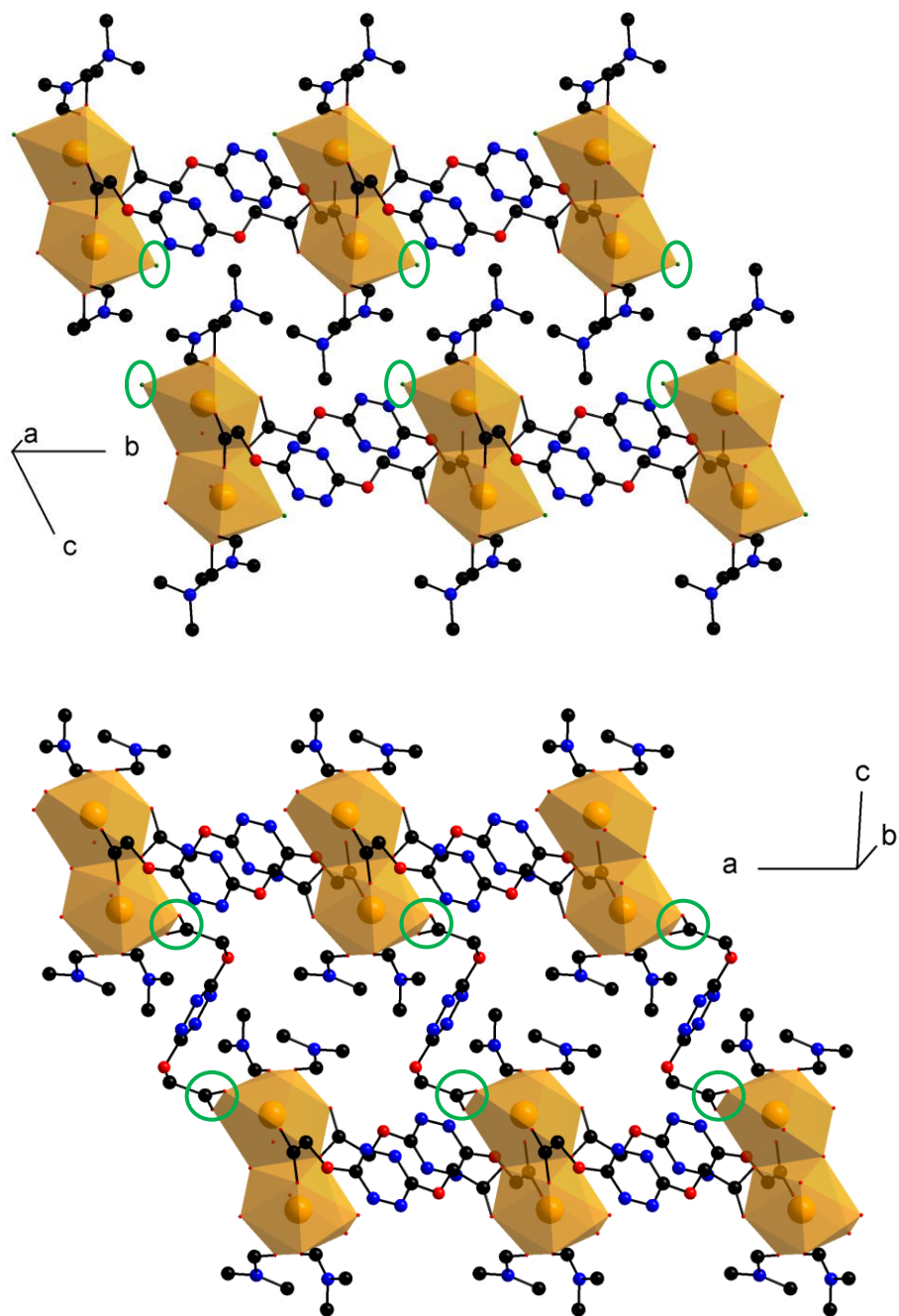
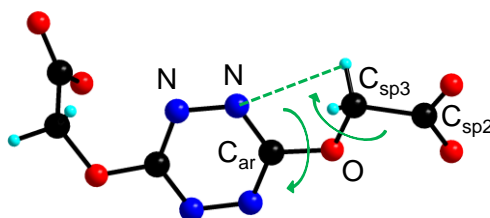


Figure S10. Relationship between the crystal structure of a) MIL-165(Tb) and b) MIL-166(Tb). Green circles highlight the substituted chloride ions and newly introduced carboxylate groups in MIL-165(Tb) and MIL-166(Tb) respectively. H atoms omitted for the sake of clarity.

Table S2. Geometry of OTz: bond distances (Å) and dihedral angles (°) in H₂OTz, MIL-164, MIL-165 and MIL-166. * Average value; # centrosymmetric molecule; § shortest distance. The low precision on the values related to MIL-165(Tb) and MIL-166(Tb) is associated with the poor quality of the diffraction datasets.



	N-N	N-C _{ar}	C _{ar} -O	O-C _{sp3}	C _{sp3} -C _{sp2}	N...H [§]	N-C-O-C	C-O-C-C
H₂OTz[#]	1.321(1)	1.334(1) 1.331(1)	1.335(1)	1.429(1)	1.505(1)	2.410	0.8(4)*	77.34(9)
MIL-164(La)	1.335(8) 1.322(7)	1.334(8) 1.338(8) 1.317(8) 1.339(8)	1.340(8) 1.342(8)	1.429(8) 1.436(8)	1.507(8) 1.521(8)	2.495 2.419	9.5(10)* 10.2(4)*	67.9(7) 72.1(7)
MIL-165(Tb)	1.31(3) 1.30(2)	1.32(3) 1.33(3) 1.33(3) 1.33(3)	1.34(3) 1.33(3)	1.38(3) 1.46(2)	1.53(3) 1.56(3)	2.532 2.472	15(2)* 4(3)*	9(2) 68(3)
MIL-166(Tb)								
Ligand A	1.32(1) 1.29(1)	1.34(1) 1.34(1) 1.32(1) 1.35(1)	1.32(1) 1.32(1)	1.43(1) 1.43(1)	1.50(1) 1.51(1)	2.532 2.495	9(1)* 11(3)*	1(1) 64(1)
Ligand B[#]	1.32(2)	1.33(2) 1.32(2)	1.33(1)	1.43(1)	1.54(2)	2.428	10(8)*	66(2)

Table S3. Tb...Tb distances in MIL-165(Tb) and MIL-166(Tb).

	intra-dimer (Å)	inter-dimer (Å)	inter-chain (Å)
MIL-165(Tb)	3.971(3)	10.802(6)	8.251(5)
MIL-166(Tb)	4.019(2)	10.177(3)	11.126(4)
variation (%)	-1.2	5.8	34.8

3. Infrared (IR) spectroscopy

Room temperature IR spectra (Figures S11, S12 and S13) were collected on a Nicolet Magna-IR 6700 Thermo Scientific spectrometer between 500 and 4000 cm^{-1} .

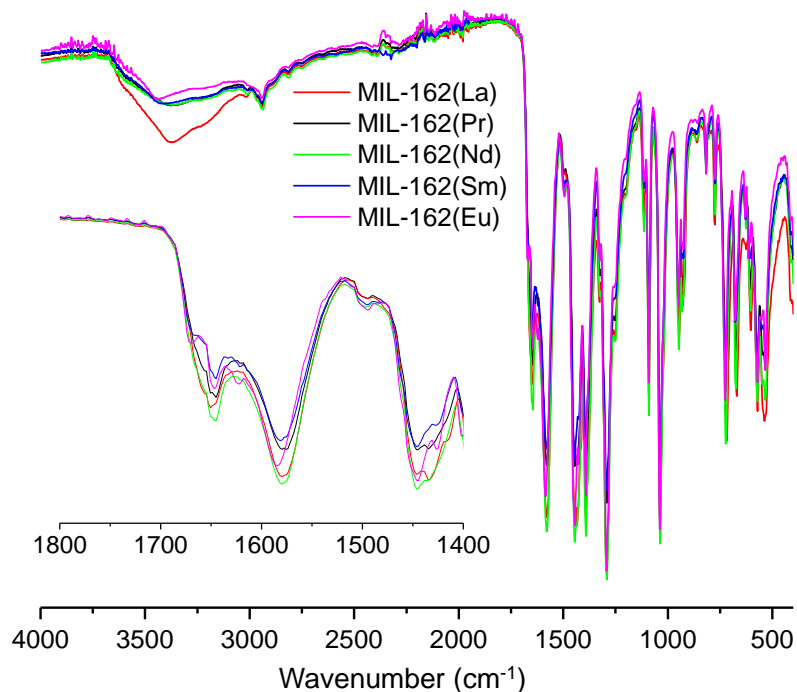


Figure S11. IR spectra of the as-synthesized MIL-162(Ln) (Ln = La, Pr, Nd, Eu). Inset: zoom on the 1800-1400 cm^{-1} region.

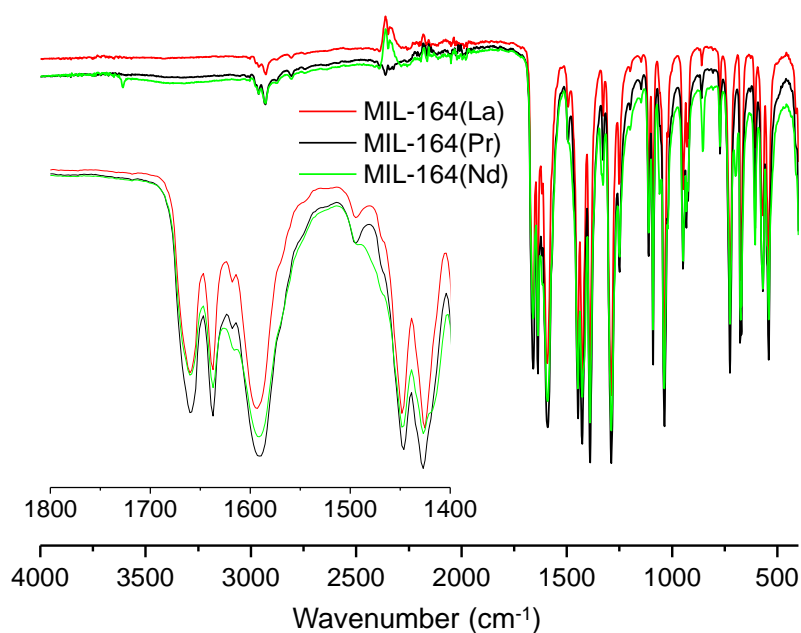


Figure S12. IR spectra of MIL-164(Ln) (Ln = La, Pr, Nd). Inset: zoom on the 1800-1400 cm^{-1} region.

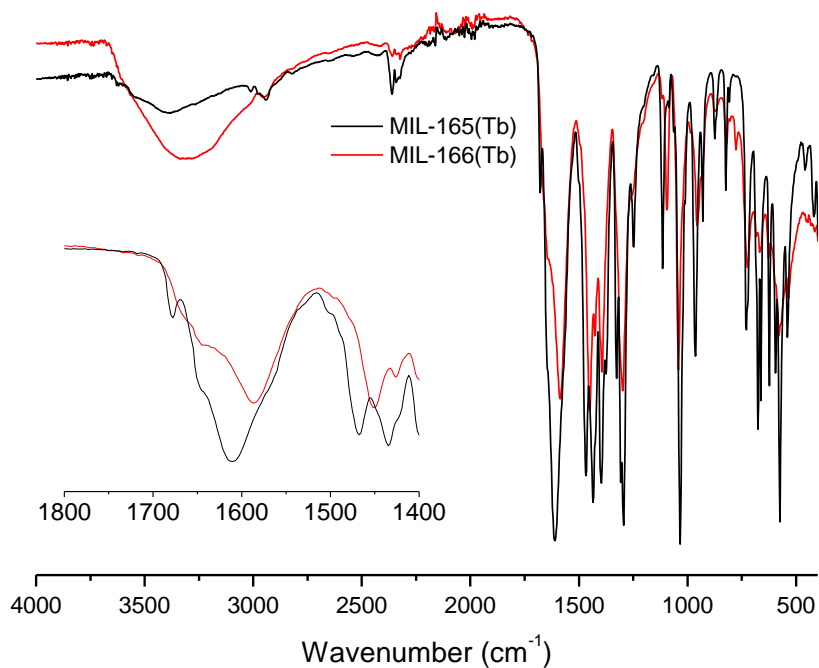


Figure S13. IR spectra of MIL-165(Tb) and MIL-166(Tb). Inset: zoom on the 1800-1400 cm^{-1} region.

4. Thermogravimetric analysis (TGA)

TGA (Figure S14) was performed on Mettler Toledo TGA/DSC 1, STAR®System apparatus under O_2 atmosphere, at a heating rate of $3\text{ }^\circ\text{C min}^{-1}$ up to $600\text{ }^\circ\text{C}$. Experimental and theoretical weight losses extracted from the proposed formula are summarized in Table S4.

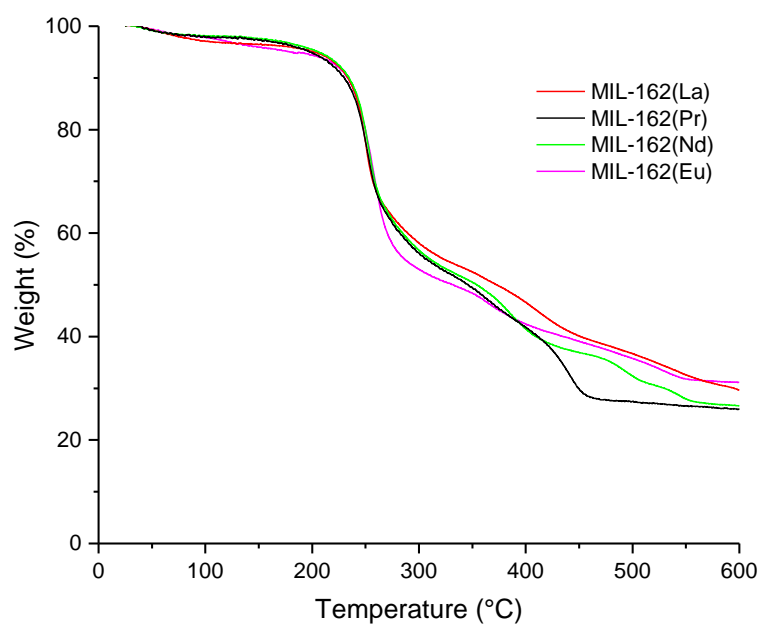


Figure S14. TGA of MIL-162(Ln), Ln = La, Pr, Nd, Eu.

Table S4. Experimental and theoretical remaining weight at 600°C for MIL-162(Ln) or $\text{Ln}_2(\text{OTz})_3(\text{DMF})_n$. Calculations were carried out for both $n = 2$ and $n = 4$ assuming that the final products are Ln_2O_3 .

Ln	Measured	Calculated (n = 4)	Calculated (n = 2)
La	29.7	25.8	29.4
Pr	25.9	26.1	29.6
Nd	26.6	26.5	30.1
Eu	31.2	27.4	31.0

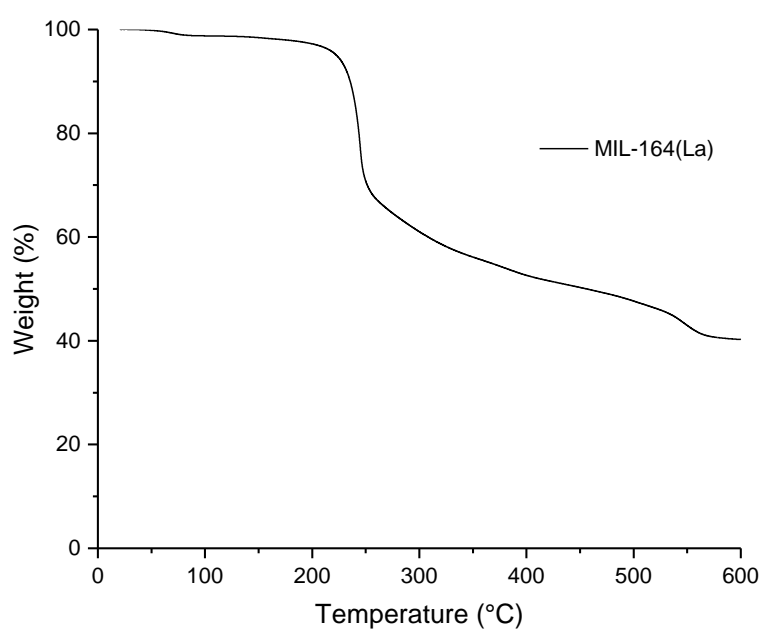


Figure S15. TGA of MIL-164(La).

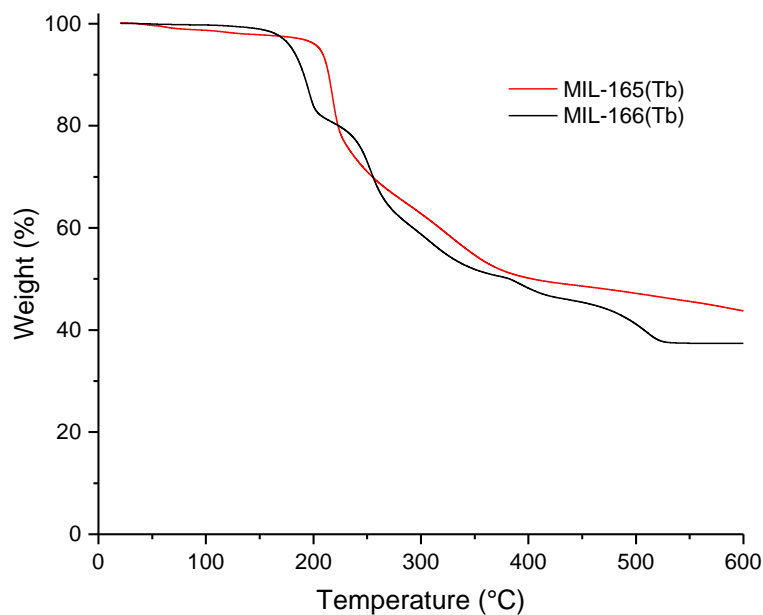


Figure S16. TGA of MIL-165(Tb) and MIL-166(Tb).

5. Elemental analysis

Chemical analysis were carried out at the ‘Institut de Chimie des Substances Naturelles’ (Gif sur Yvette, France).

- MIL-162(La) or $\text{La}(\text{C}_6\text{H}_4\text{N}_4\text{O}_6)_{1.5}(\text{C}_3\text{H}_7\text{NO})$. Exp. wt. C 24.1 %, H 2.8 %, N 16.7 %; Calc. wt. C 26.0 %, H 2.4 %, N 17.7 %.

- MIL-164(La) or $\text{LaCl}(\text{C}_6\text{H}_4\text{N}_4\text{O}_6)(\text{C}_3\text{H}_7\text{NO})_2$. Exp. wt. C 25.3 %, H 3.3 %, N 15.0 %; Calc. wt. C 26.3 %, H 3.3 %, N 15.3 %.

- MIL-165(Tb) or $\text{TbCl}(\text{C}_6\text{H}_4\text{N}_4\text{O}_6)(\text{C}_3\text{H}_7\text{NO})_2$. Exp. wt. C 22.6 %, H 3.0 %, N 13.6 %; Calc. wt. C 25.3 %, H 3.2 %, N 14.8 %.

- MIL-166(Tb) or $\text{Tb}(\text{C}_6\text{H}_4\text{N}_4\text{O}_6)_{1.5}(\text{C}_3\text{H}_7\text{NO})_2$. Exp. wt. C 27.1 %, H 3.3 %, N 16.2 %; Calc. wt. C 27.8 %, H 3.1 %, N 17.3 %.

6. Optical experiments

- General conditions

For all solids (MIL-162 to MIL-166), an ethanolic suspension with a concentration of 0.22 g L^{-1} was prepared. The suspensions were stirred within the quartz cell during the measurement to insure their homogeneity. The properties of the free H_2OTz ligand were evaluated from solution with optical densities <0.1 at the excitation wavelength and below, in order to avoid reabsorption artifacts, in ethanol. The UV-Vis absorption spectrum of H_2OTz (Figure S15) was measured on a Varian CARY 5000 spectrophotometer. Emission spectra were measured on a Fluorolog-3 (Horiba Jobin-Yvon) spectrofluorimeter. A right-angle configuration was used. Absolute quantum yields measurements of coordination polymers suspensions were performed using an integrating sphere (Horiba Jobin-Yvon).

- UV-Vis absorption and steady state fluorescence

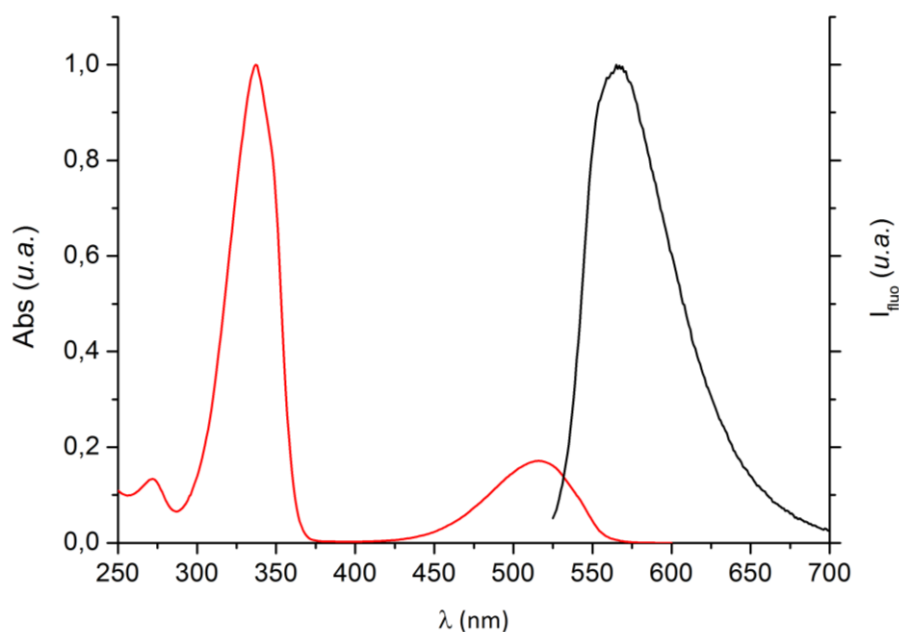


Figure S17. UV-visible absorption spectrum of H_2OTz (red) and emission spectrum (black) after excitation at 520 nm.

Time resolved fluorescence

The fluorescence decay curve of H₂OTz (Figure S16) was obtained with the time-correlated single-photon-counting method using a Spectra-Physics titanium-sapphire Tsunami laser pumped by a Millennia Xs laser (82 MHz, repetition rate lowered to 4 MHz thanks to a pulse-picker, around 500 fs pulse width, a doubling crystal is used to reach 409 nm excitation). Fluorescence photons are detected at 90°, through a long pass filter and a monochromator, with a Hamamatsu MCP photomultiplier R3809U. The data were acquired using a SPC-630 TCSPC system (Becker & Hickl GmbH). The analysis is performed with the Globals software from Laboratory for Fluorescence Dynamics (LFD) at the University of Illinois at Urbana-Champaign. The decay curve of H₂OTz $I(t)$ could satisfactorily be fitted by the following exponential curve, leading to a life time $\tau = 76$ ns.

$$I(t) = A \cdot \exp\left(-\frac{t}{\tau}\right)$$

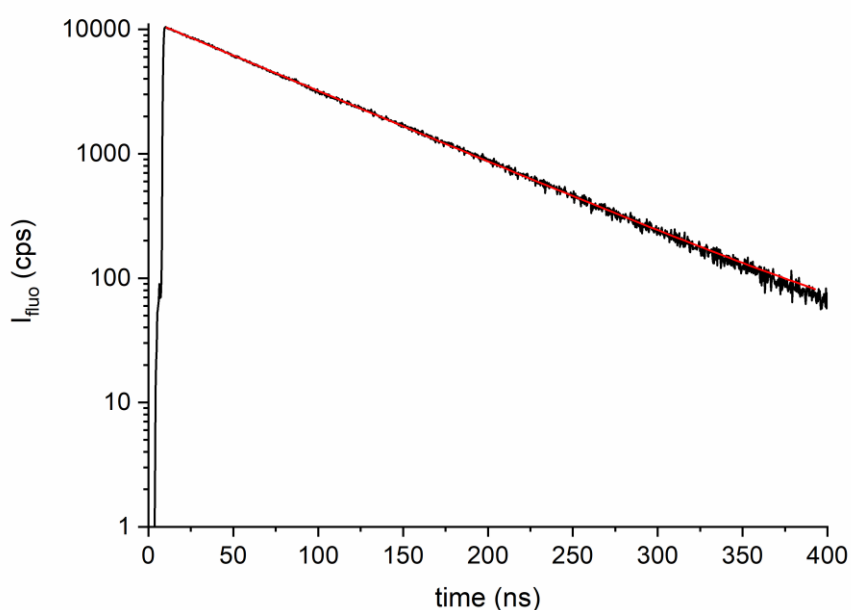


Figure S18. Experimental (black) and calculated (red) fluorescence decay curves of H₂OTz in ethanol.

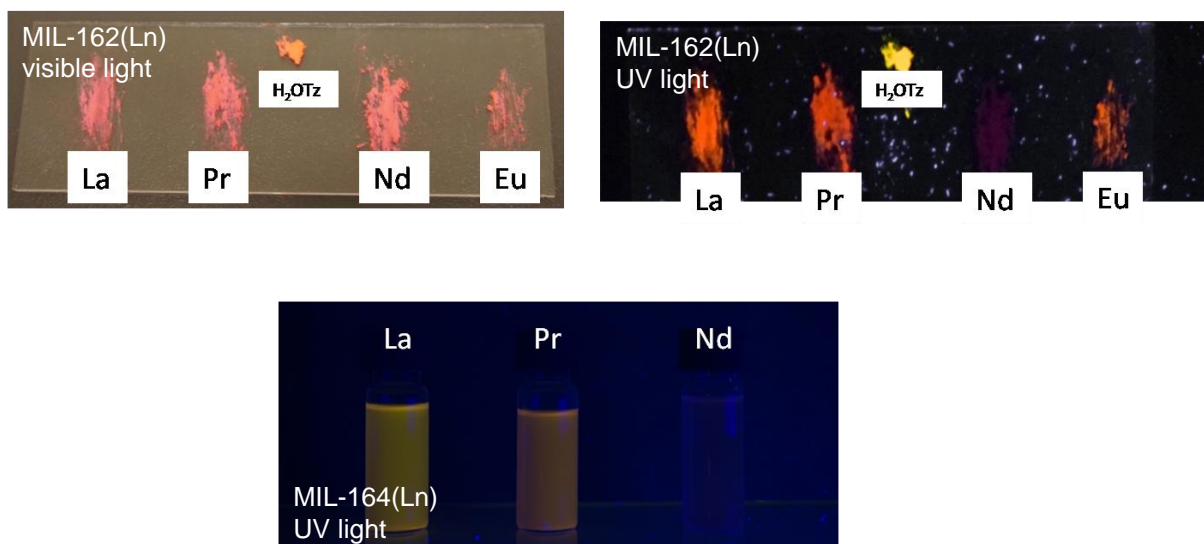


Figure S19. Top: picture of powdered H₂OTz and MIL-162(Ln) (Ln = La, Pr, Nd, Eu) deposited on a glass slice under visible (left) and UV (365 nm, right) light irradiation; bottom: picture of MIL-164(Ln) (Ln =La, Pr, Nd) suspended in ethanol under UV (365 nm) light irradiation.

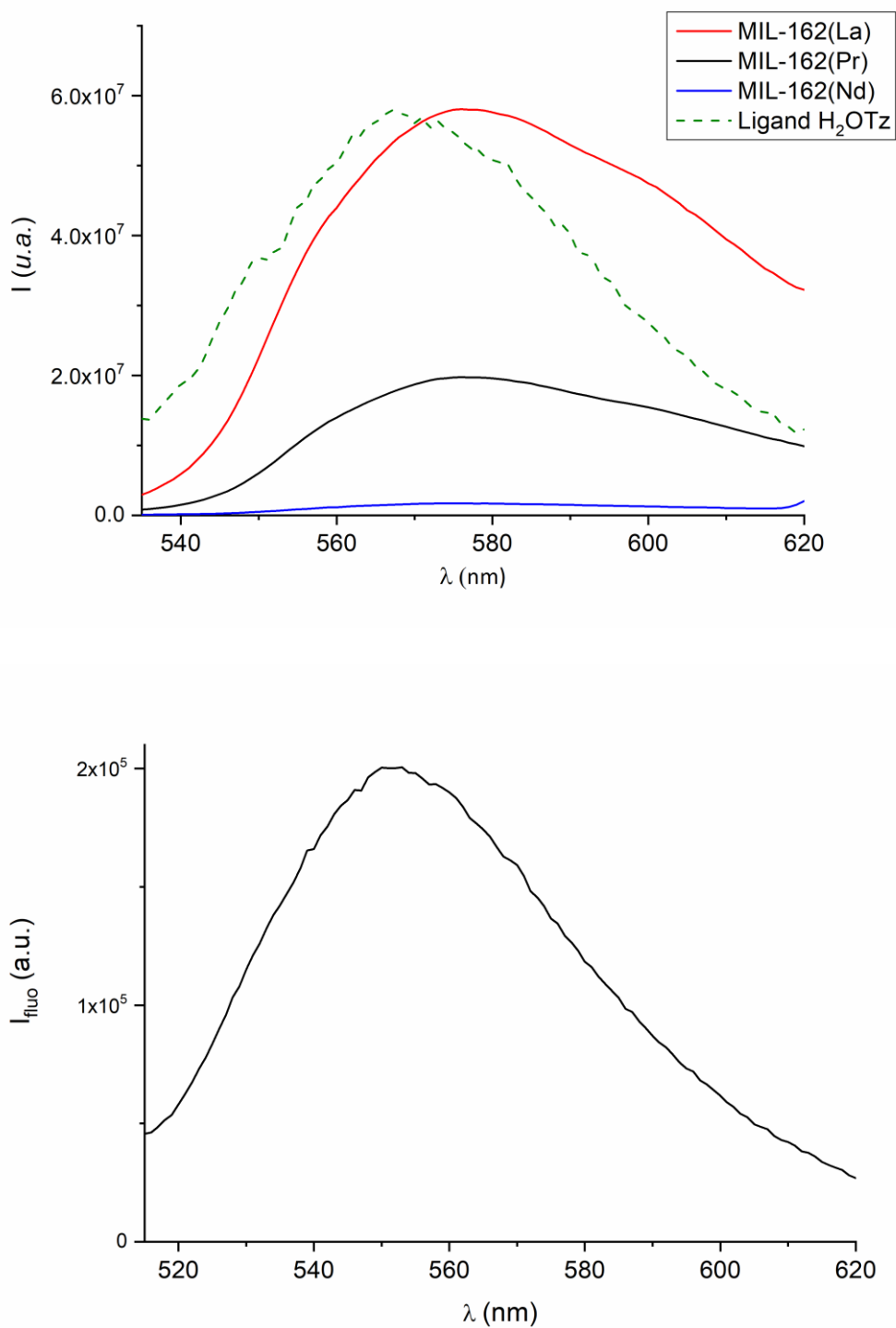


Figure S20. Fluorescence emissions spectra of MIL-162(Ln) solids in ethanol suspensions compared with the one of H₂OTz in the powder state (top) and of MIL-165(Tb) in ethanol suspension (bottom). Excitation wavelength 320 nm.

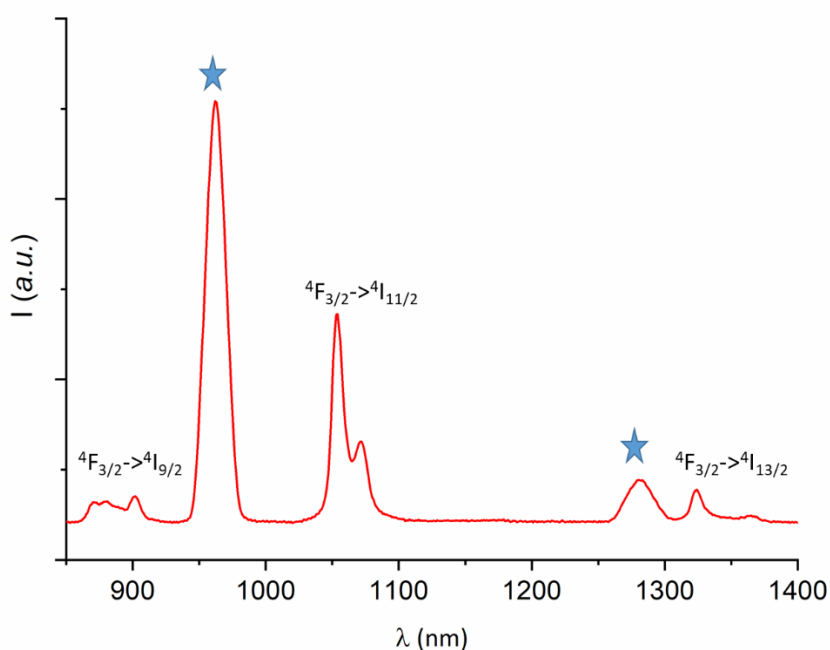


Figure S21. Fluorescence emission spectrum in the near IR region of a suspension of MIL-164(Nd). The stars indicate third and fourth harmonics of the excitation wavelength (320 nm).

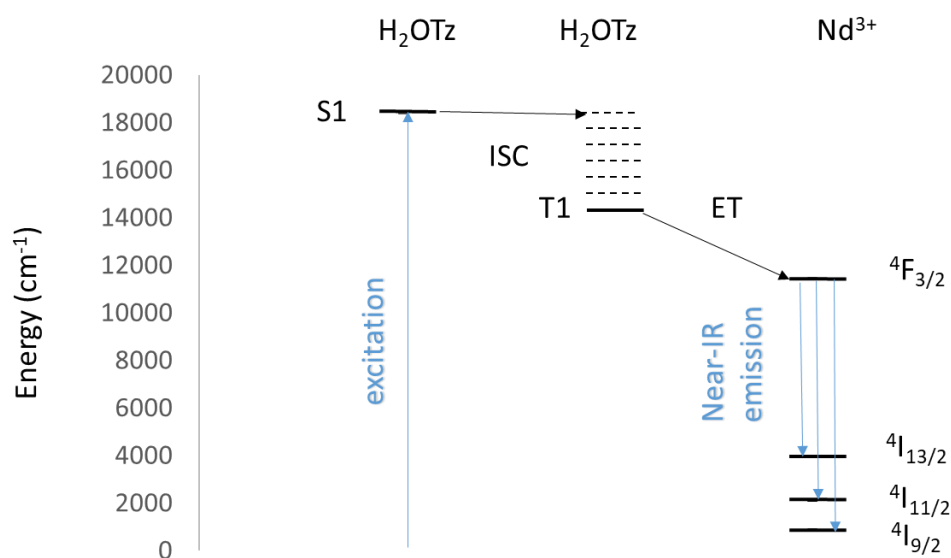


Figure S22. Schematic energy transfer diagram from the tetrazine OTz to the Nd^{3+} cation

References

- [1] J. Jurayj, M. Cushman, *Tetrahedron* **1992**, *48*, 8601–8614.
- [2] M. D. Helm, A. Plant, J. P. A. Harrity, *Org. Biomol. Chem.* **2006**, *4*, 4278–4280.
- [3] G. M. Sheldrick, *Acta Crystallogr. Sect. C Struct. Chem.* **2015**, *71*, 3–8.
- [4] A. L. Spek, *Acta Crystallogr. Sect. C Struct. Chem.* **2015**, *71*, 9–18.